Modeling and Simulation of a Thermoelectric Heat Exchanger using the Object-Oriented Library TIL

Christine Junior, Christoph Richter, Wilhelm Tegethoff, Nicholas Lemke, Jürgen Köhler
Institut für Thermodynamik, TU Braunschweig, Germany
c.junior@tu-bs.de ch.richter@tu-bs.de

Abstract

Thermoelectric technology allows for the direct conversion of a temperature difference into an electric potential and vice versa. Thermoelectric devices can act as coolers, heaters, or power generators and applications of small capacity thermoelectric modules are widespread. Applications of large capacity thermoelectric devices have been limited for decades by their low efficiency. New environmental regulations regarding the manufacture and release of CFCs have revived the interest in this area. Recent investigations on thermoelectric materials promise that their thermoelectric efficiency can be improved dramatically. This would mean a breakthrough for new fields of applications for thermoelectric modules. A new Modelica model of a Peltier water-water heat exchanger was developed for transient simulations. The new model uses component models from the object-oriented Modelica library TIL. The new model was used to simulate the transient behavior of a Peltier heat exchanger during a sudden reversion of the applied voltage. The numerical results were compared to measurement results from a prototype.

Keywords: heat exchanger; simulation; thermoelectrics; Peltier element

1 Introduction

Thermoelectric technology allows for the direct conversion of a temperature difference into an electric potential and vice versa. The French physicist Jean Peltier discovered in 1834 that an electric current sent through a circuit made of dissimilar conducting materials yields heat absorption at one junction and heat rejection at the other. Standard thermoelectric modules utilize doped bismuth telluride as semiconductor and achieve moderate performance. They can act as coolers, heaters, or power generators and applications of small capacity thermoelectric modules are widespread. However applications of large capacity thermoelectric devices have been limited in the past by the low efficiency of thermoelectric modules. Recent scientific advances regarding new materials and assembly methods for thermoelectric modules as well as the increasing concerns about fuel economy, harmful emissions of particulate matter, and chemical refrigerants revived the interest in thermoelectric technology. The inherent advantages of thermoelectric systems such as the absence of moving parts, quiet operation, and environmental friendliness of the module itself have further increased the interest. Several investigations for applications of large capacity thermoelectric modules in the fields of refrigeration and air-conditioning [1], waste heat recovering [2], or superconduction [3] have been carried out with promising results.

This paper describes the development of a Modelica model that allows the transient simulation of thermoelectric devices to determine their performance potential. The model for the thermoelectric devices was developed as an add-on for the object-oriented Modelica library TIL (TLK-IfT-Library) described in [4] that allows for the simulation of thermodynamic systems such as air-conditioning and heat-pump systems.

2 Thermoelectric Refrigeration

Thermoelectric refrigeration is achieved when a direct current I is passed through one or more pairs of n-type and p-type semiconductors connected with a metal with high conductivity such as copper as sketched in Figure 1.

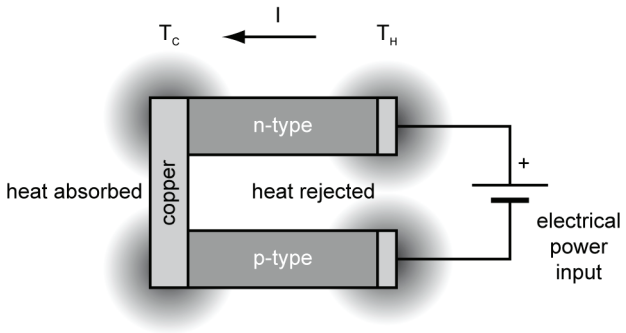

Figure 1: The Peltier effect (thermoelectric cooling) from [5].

If the electric current passes from the n-type to the p-type semiconductor, electrons pass from a low energy level in the p-type material through the interconnecting conductor to a higher energy level in the n-type material. Thus the temperature T_C of the interconnecting conductor decreases and heat is absorbed from the environment. The absorbed heat is transferred by electron transport through the semiconductors to the other end of the function. It is liberated as the electrons return to a lower energy level in the p-type material yielding an increased temperature T_H.

This phenomenon is known as the Peltier effect and is described by the Peltier coefficient π, defined as the product of the Seebeck coefficient α of the semiconductor material and the absolute temperature. The Peltier coefficient relates to a cooling effect as the electric current passes from the n-type to the p-type semiconductor and a heating effect as the polarity of the power supply is changed. Reversing the direction of the electric current also reverses the temperatures of the hot and cold ends.

The amount of heat absorbed at the cold end not only depends on the product of the Peltier coefficient and the electric current flowing through the thermoelectric module but also on two other effects: Due to the temperature difference between the cold and the hot ends of the semiconductors, heat is conducted through the semiconducting material from the hot to the cold end. The amount of conducted heat depends on the thermal conductance κ of the material as well as on the temperature difference. The second effect occurs when the electric current is passing through the semiconductors. The electrical resistance R causes the generation of the so-called Joule heat in equal shares at the cold and the hot side of the thermoelectric device. The Joule heat is dependent on the electrical resistance and proportional to the square of the electric current and therefore becomes eventually the dominant factor.

The heat absorption rate at the cold side of the thermoelectric module can be described taking into account the three different effects mentioned above

$$\dot{Q} = \alpha T_C I - \frac{1}{2} I^2 R - \kappa (T_H - T_C)$$

where α is the differential Seebeck coefficient sometimes referred to as α_{pn}, R the electrical resistance of the thermoelements in series, and κ the thermal conductance of the thermoelements in parallel. The energy efficiency of the thermoelectric device is described by its coefficient of performance (COP) defined as the net heat absorbed at the cold junction divided by the electric power input

$$COP = \frac{\dot{Q}}{P_{el}} = \frac{\alpha T_C I - \frac{1}{2} I^2 R - \kappa \Delta T}{\alpha \Delta T I + I^2 R}$$

The refrigeration capability of a semiconductor material depends on a combined effect of the Seebeck coefficient α, the electrical resistivity ρ, and the thermal conductivity κ of the material over the operational temperature range between the cold and the hot junctions. The electrical resistivity is defined as

$$\rho = R \frac{A}{l}$$

where A is the cross-sectional area of the resistive material and l its length. The three material properties are combined in the thermoelectric figure of merit Z defined as

$$Z = \frac{\alpha^2}{\kappa \rho}$$

The figure of merit is used by material scientists to describe the efficiency of semiconductor materials for thermoelectric applications.

3 Prototype Peltier Heat Exchanger

The Peltier effect can be used for heating and cooling in practical applications by combining thermoelectric modules with conventional heat exchangers. The fluid flowing through the heat exchanger acts as a heat sink at the hot side of the thermoelectric module and as a heat source at the cold side. Figure 2 shows the assembly of the prototype Peltier heat exchanger used for all measurements.

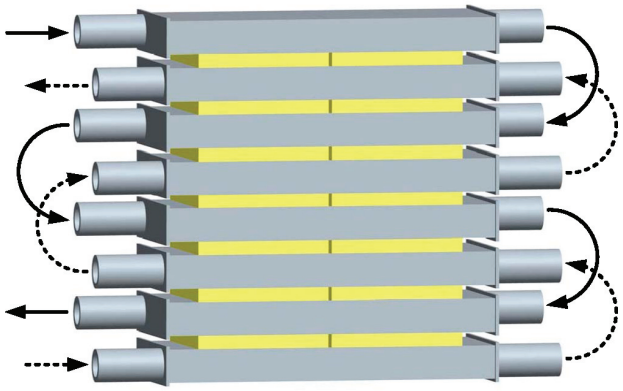

Figure 2: CAD drawing of the prototype Peltier water-water heat exchanger. The Peltier elements are the flat cuboids between two aluminum channels. The orientation of the Peltier elements changes successively between the rows of channels.

Because of the consolidated design and small size of the prototype heat exchanger, water was chosen as coolant at both sides. The heat exchanger consists of rectangular aluminum channels whose endings are covered by plates. Aluminum cores act as connecting tubes. The prototype heat exchanger is assembled so that both sides of the thermoelectric module are in contact with a channel. The arrangement of the thermoelectric modules has to be taken into account for an efficient utilization of the Peltier effect. It is necessary to either heat or cool the channels. A combination of heating and cooling does not yield a reasonable application.

To increase the flow velocity and the heat exchange between the fluid and the wall, three barriers were installed in each channel. A CFD simulation was carried out to determine the flow situation in the channel. The simulations results proved that the fluid meanders through the channel and showed that fluid circulation caused by the barriers leads to a decrease in dead storage capacity and thus to an improvement in the heat exchange between fluid and wall. Figure 3 shows a single channel and the corresponding flow path.

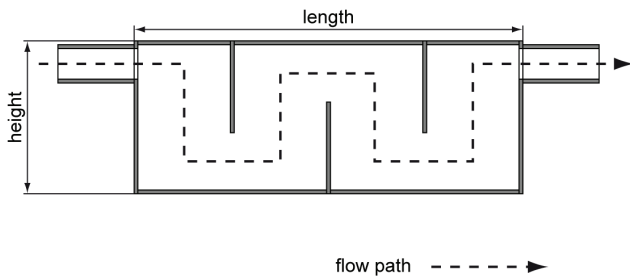

Figure 3: Single channel element of prototype Peltier heat exchanger.

4 Heat Exchanger Model

In order to model the prototype Peltier heat exchanger, a model for a Peltier element had to be developed. The new model was developed based on the component model library TIL (TLK-IfT-Library) that contains models for a steady-state and transient simulation of thermodynamic systems (see [4] for more information).

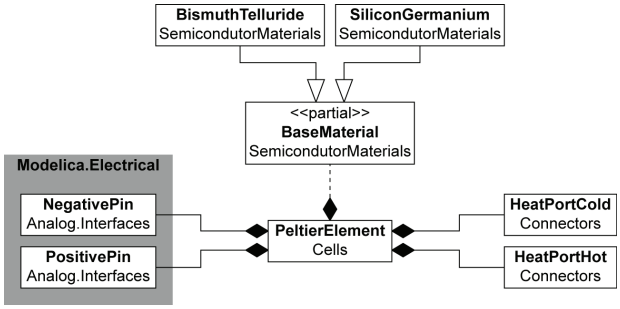

Figure 4: UML class diagram of PeltierElement.

Figure 4 shows a class diagram of the new model PeltierElement. The material properties of the semiconductor material are stored in a record extending from BaseMaterial. Two heat ports derived from the HeatPort connector defined in TIL and two electric pins defined in the Modelica Standard Library are the interface of the PeltierElement. Based on the equations presented in Section 2, the following set of equations is used to describe the Peltier element

$$I_{negative} + I_{positive} = 0$$

$$U_{positive} - U_{negative} = RI_{negative}$$

$$P_{el} + \dot{Q}_C + \dot{Q}_H = 0$$

$$COP = \frac{\alpha T_C I - 1/2\, I^2 R - \kappa(T_H - T_C)}{\alpha \Delta T I + I^2 R}$$

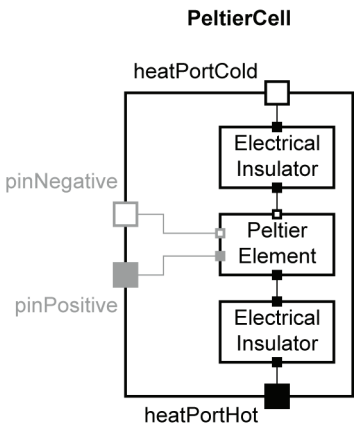

Figure 5: PeltierCell model as defined in TIL_AddOn_ThermoElectrics.

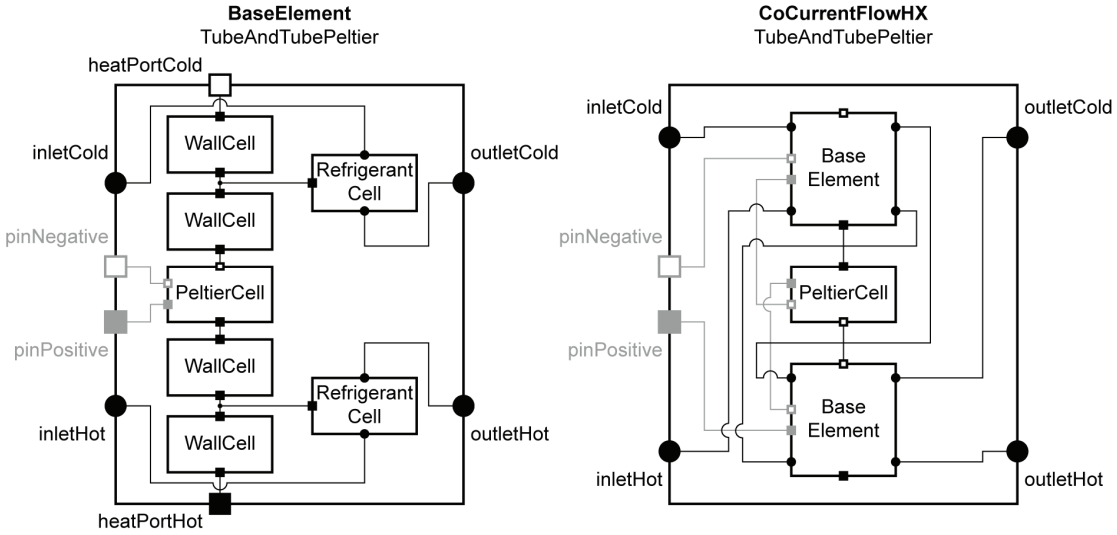

Figure 6: BaseElement and its usage in a Peltier water-water heat exchanger model from TIL_AddOn_ThermoElectrics. The PeltierCell is shown in Figure 5.

$$\dot{Q}_C = -COP \cdot P_{el}$$
$$\dot{Q}_H = (1 + COP) \cdot P_{el}$$

The PeltierElement is instantiated in the PeltierCell model along with two models for electrical insulators as shown in Figure 5. The electrical insulators prevent a short circuit between the Peltier elements and the aluminum channels. Note that the naming of the heat ports in Figure 5 is chosen for the default case that is a positive electric current in the conventional current notation. The hot side eventually becomes the cold side and vice versa if the direction of the current is reversed. The swapping of the corresponding temperatures T_C and T_H is implemented using a smooth transition function with a very short transition period.

In order to model the prototype Peltier heat exchanger shown in Figure 2 in a flexible way, an additional model called BaseElement is introduced that models a single layer of the heat exchanger.

A layer consists of two aluminum channels as sketched in Figure 3 and the Peltier element in between those two channels. The model is illustrated in the left picture in Figure 6. A refrigerant cell and two wall cells from TIL are combined to model a single channel. The reason for using a RefrigerantCell instead of a LiquidCell is that the new heat exchanger model was developed to cover cases of evaporating

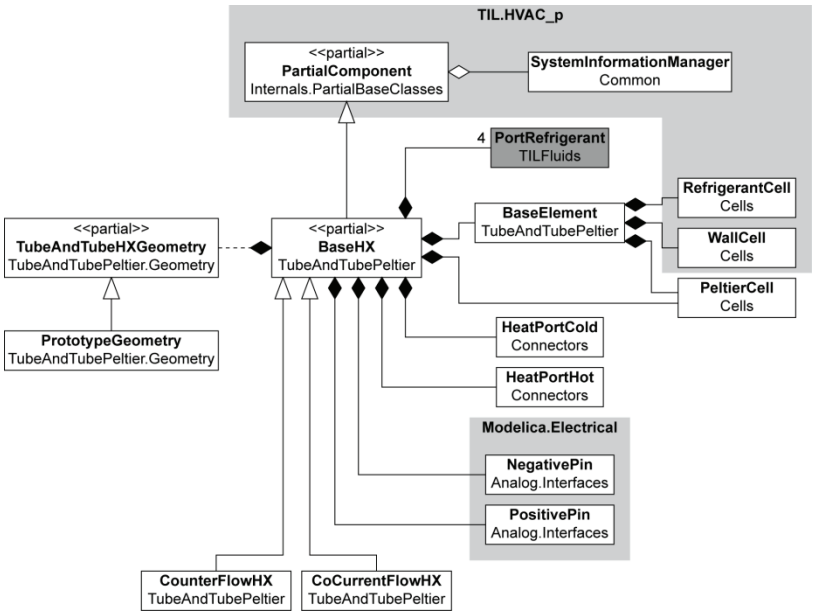

Figure 7: UML class diagram of TubeAndTubePeltier heat exchanger in TIL_AddOn_ThermoElectrics. The wall material model and all heat transfer and pressure drop models are skipped for simplicity.

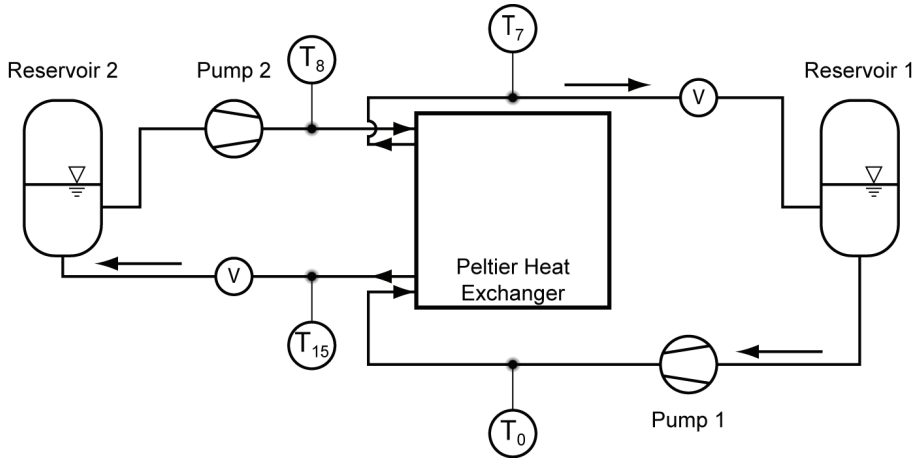

Figure 8: Schematic diagram of Peltier heat exchanger test stand.

and condensing fluids in both fluid paths. The two channels are connected using a PeltierCell as shown in Figure 5. Note that the BaseElement model in Figure 6 can directly be used as a single cell heat exchanger model.

The model for the Peltier heat exchanger assembles instances of BaseElement and PeltierCell as shown in the right picture in Figure 6. The prototype heat exchanger shown in Figure 2 for example is composed of four base elements and three Peltier cells in between. Figure 7 shows the class diagram of the new TubeAndTubePeltier heat exchanger model. Note that the wall material model and all heat transfer and pressure drop models are skipped for simplicity. A more detailed description of the structure of heat exchanger models in TIL is given in [4].

5 Measurements

A series of measurements was carried out with the prototype Peltier water-water heat exchanger presented in Section 3. Figure 8 shows a schematic diagram of the test stand used for all measurements.

To ensure a constant temperature at the water inlet of the prototype, a reservoir was used in both cycles. Water was pumped from the reservoirs into the prototype and flowed back after running through the heat exchanger. The reservoirs were chosen large enough to prevent significant temperature changes during operation. The volume flow rates were regulated with appropriate throttling devices and measured by using conventional water meters.

Besides the volume flow rates characteristic parameters such as the water temperatures at the inlet and outlet of each aluminum tube or the electric current and voltage dropping out over every Peltier element were taken up. The boundary conditions for the measurements were selected in consideration of showing the applicability of the simulation for different premises. Therefore a low, a medium and a high water inlet temperature were chosen and each condition measured by using a low and a high volume flow rate respectively. Each measurement was carried out at a working-voltage of 10 V. A summary of the boundary conditions for all measurements is given in Table 1.

	Water Stream 1		**Water Stream 2**	
#	V_1 [l/min]	T_0 [°C]	V_2 [l/min]	T_8 [°C]
1	2.05	4.00	2.00	4.00
2	0.90	4.00	0.85	4.00
3	2.20	18.00	2.10	18.00
4	0.85	18.00	0.80	18.00
5	2.35	30.00	2.40	30.00
6	1.00	30.00	1.10	30.00

Table 1: Measurements with prototype Peltier water-water heat exchanger.

All measurements were carried out in the same way: After reaching a stationary point for the boundary conditions listed in Table 1, the direction of the electric current was changed from positive to negative in the conventional current notation. The resulting change in temperature was detected until the values became stationary again.

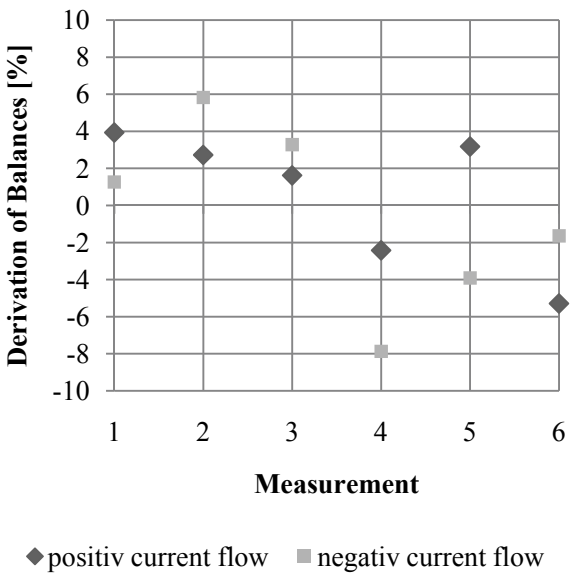

Figure 9: Deviation of electrical and thermal balances for all measurement points.

An evaluation of the quality of the measurements was carried out by comparing the sum of the input power and the gained cooling capacity to the achieved heating capacity according to

$$P_{el} + \dot{Q}_{cooling} = \dot{Q}_{heating}$$

The cooling capacity as well as the heating capacity was calculated from

$$\dot{Q} = \dot{m} c_p \Delta T$$

and the electric power from

$$P_{el} = U \cdot I$$

The deviation within the balance has to be zero for the ideal case. The deviation of the two balances for each measurement is shown in Figure 9. It can be seen that the deviation lies between 1% and 8%, and that the average value lies around 4%. A connection between the direction of the electric current and the resulting deviation can not be identified.

To exclude the existence of a statistical error and to confirm that the deviations of the balances are lying within the measuring accuracy an error analysis was carried out. Therefore, Gauss' error propagation law was used according to

$$\Delta\bar{F} = \sqrt{\left(\frac{\partial F}{\partial x}\Delta\bar{x}\right)^2 + \left(\frac{\partial F}{\partial y}\Delta\bar{y}\right)^2 + \cdots}$$

Measurement 4 from Table 1 was selected for an error analysis exemplarily. A variation of relevant measurands was carried out to find out the impact of these measurands on the total error and to identify possible potentials for further optimization.

Figure 10 shows the impact of the error occurring during the measurement of the temperature difference ΔΔT between the inlet and outlet of the Peltier prototype heat exchanger and during the estimation of the volume flow rate ΔV on the resultant heating or cooling capacity.

Due to the fact that the measuring accuracy of a thermocouple lies at about 0.3 K, the maximum error for the mathematical calculation of the temperature difference can be expected to be 0.6 K when using temperatures measured with two independent thermocouples. This error can be reduced to 0.1 K if the temperature difference is measured using two thermocouples connected in series which was done for all measurements presented in Table 1.

In consideration of the volume flow rate, measurements the deviation of the values estimated with conventional flow meters and the actual values lies between 4% and 9% which results in a maximum deviation of 0.09 l/min. The concluding summation yields - under consideration of these conditions - to

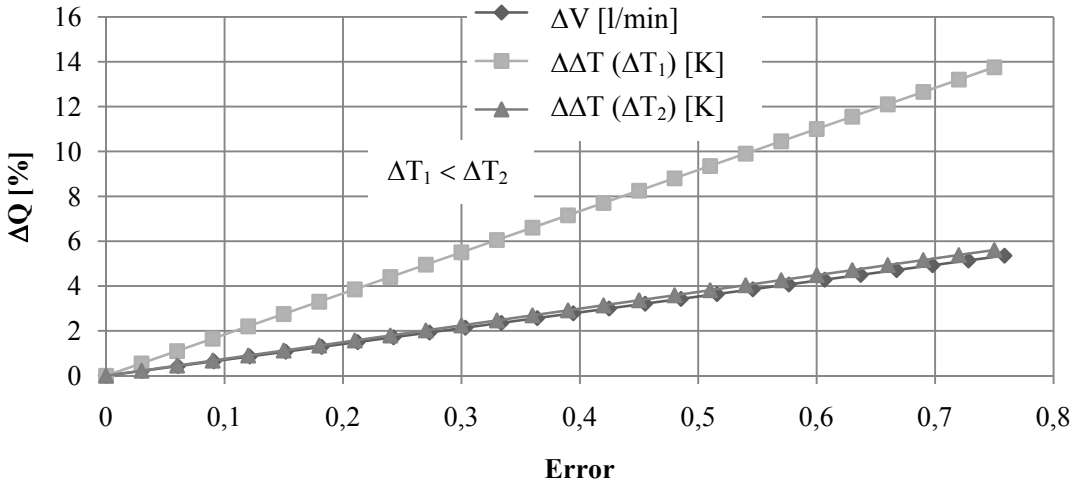

Figure 10: Error for Measurement 4 from Table 1. The corresponding units are given in the key.

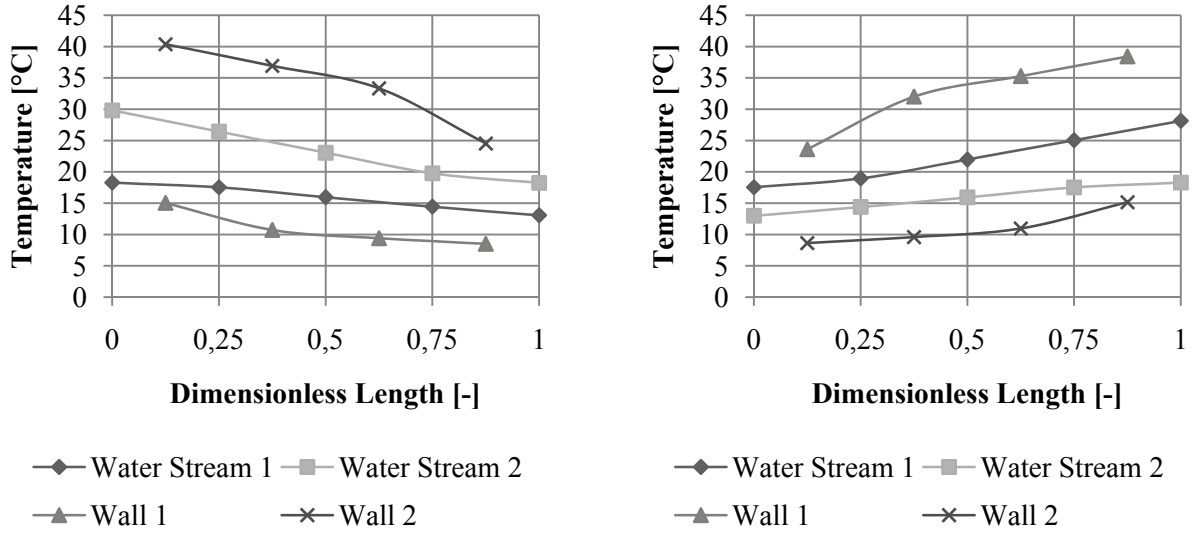

Figure 11: Temperature distribution in prototype Peltier heat exchanger before and after reversion of the applied voltage for Measurement 4 from Table 1.

the result that even the measurements with a deviation of balances of 8% are lying within measuring accuracy.

6 Simulation

Simulations were carried out for all measurements listed in Table 1. Measurement values were used for the electric current, for the two volume flow rates, and for the water temperatures T_0 and T_8 at the two heat exchanger inlets. The Peltier modules used in the prototype Peltier heat exchanger are standard bismuth telluride modules without any further specification from the manufacturer. Constant properties for the Seebeck coefficient α and the thermal conductance κ taken from Rowe [5, Table 9.1] were used in the Peltier element model. The electrical resistance R of the thermoelectric module was not specified by the manufacturer and had to be determined from the measurements. The reversion of the applied voltage was implemented using a smooth transition function with a period of Δt = 1s. This section describes the results obtained for the simulation of Measurement 4 from Table 1. A constant coefficient of heat transfer α = 4,100 W/m^{2}K was used. This coefficient of heat transfer was determined based on a CFD simulation of the flow through a single aluminum channel.

Figure 11 shows the temperature distribution in the prototype Peltier heat exchanger before and after the reversion of the applied voltage. The numbering of the water streams and of the walls refers to the numbering of the two independent water circuits as presented in Figure 8. The water temperatures are shown for the inlet of each channel and for the outlet of the last channel for both water streams. The wall temperatures are averages of the temperatures in the center of both wall cells connected to the same refrigerant cell as shown in Figure 6.

Figure 11 shows that the temperature change in the entrance channel of each water stream is smaller than in all other subsequent channels. This is caused by the fact that the entrance channels are insulated at one side and connected to a Peltier element at the other side whereas all other channels are connected to a Peltier element at both sides. The two diagrams shown in Figure 11 are mirror-symmetrical which demonstrates the reversibility of the process.

Figure 12 shows a comparison of the measured outlet temperature for each water stream with the values obtained from the transient simulation. The top picture shows the change in the electric current I caused by the reversion of the applied voltage.

Figure 12 illustrates that the simulated start and end temperatures differ from the measured temperatures. The simulated system also reacts slower to the sudden reversal of the applied voltage than the real system. Further Measurements are required to improve the model of the Peltier element that is currently based on material constants taken from the literature and the measured electrical resistance as explained in the beginning of this section.

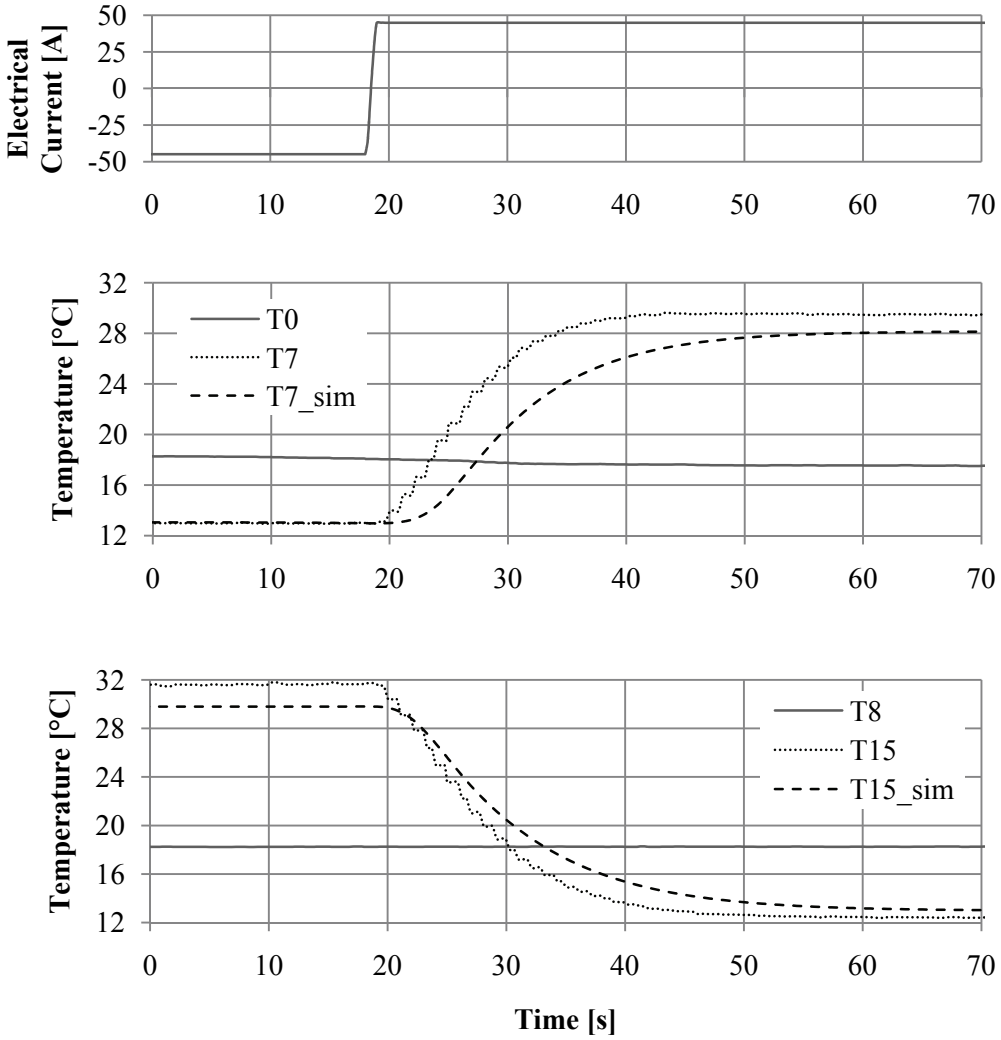

Figure 12: Measured and simulated water temperatures at inlets and outlets of prototype Peltier heat exchanger for Measurement 4 from Table 1.

7 Conclusions and Outlook

A new model for a Peltier water-water heat exchanger was presented that can be used in transient system simulations. Results from measurements with a prototype heat exchanger were used to validate the new model. Models from the new component mode library TIL [4] were used for many components of the new Peltier heat exchanger model and the new object-based fluid property library TILFluids was used to compute all fluid properties. A new model for Peltier cells was presented that was used to assemble the heat exchanger. The new heat exchanger model demonstrates that TIL can easily be extended to cover a wide range of thermodynamic systems. The presented model can be extended to cover other Peltier heat exchangers. A very interesting alternative concept to be analyzed in the future using simulations and experiments is a refrigerant-air heat exchanger with Peltier modules in between.

References

[1] J. Winkler, V. Aute, B. Yang, and R. Radermacher. Potential benefits of thermoelectric elements used with air-cooled heat exchangers. In Proc. of 2006 International Refrigeration and Air Conditioning Conference at Purdue, volume 1, pages R091.1-R091.8, West Lafayette, July 2006.

[2] K. Zorbas, E. Hatzikraniotis, and K. Paraskevopoulos. Power and Efficiency Calculation in Commercial TEG and Application in Wasted Heat Recovery in Automobile. In Proc. of 5th European Conference on Thermoelectrics, 2007.

[3] K. Bos, R. Huebener, and C. Tsuei. Prospects for Peltier cooling of superconducting electronics. Cryogenics, 38(3):325-328, March 1998.

[4] C. Richter. Proposal of New Object-Oriented Model Libraries for Thermodynamic Systems. Dissertation, TU Braunschweig, to be published in 2008

[5] D. Rowe, editor. Thermoelectrics Handbook, Macro to Nano. Taylor & Francis, 2006.